Accepted Article

May 3, 2016

Epigenome-wide DNA Methylation Analysis Implicates Neuronal and Inflammatory Signaling Pathways in Adult Murine Hepatic Tumorigenesis following Perinatal Exposure to Bisphenol A

Authors

Caren Weinhouse[1], Maureen A. Sartor[2, 3], Christopher Faulk[1], Olivia S. Anderson[1, 4], Karilyn E. Sant[1], Craig Harris[1, 4], Dana C. Dolinoy[1,4]

[1]Department of Environmental Health Sciences,[2] Department of Biostatistics, and [3]Department of Computational Medicine and Bioinformatics, [4]Department of Nutritional Sciences, University of Michigan, Ann Arbor, Michigan, USA

Corresponding author:

Dana C. Dolinoy
1415 Washington Heights
Ann Arbor, Michigan 48109-2029
Tel: 734 647-3155
Email: ddolinoy@umich.edu

Running Title: Altered DNA methylation in liver tumors from mice perinatally exposed to BPA

This is the author manuscript accepted for publication and has undergone full peer review but has not been through the copyediting, typesetting, pagination and proofreading process, which may lead to differences between this version and the Version record. Please cite this article as doi:10.1002/em.22024.

This article is protected by copyright. All rights reserved.

Abstract

Developmental exposure to the endocrine-active compound bisphenol A (BPA) has been linked to epigenotoxic and potential carcinogenic effects in rodent liver, prostate, and mammary glands. We previously reported a dose-dependent increase in hepatic tumors in 10-month mice perinatally exposed to one of three doses of BPA (50 ng, 50 µg, or 50 mg BPA/kg chow). These tumors represent early-onset disease and lack classical sexual dimorphism in incidence. Here, we investigate adult epigenome-wide liver DNA methylation profiles to identify gene promoters associated with perinatal BPA exposure and disease in 10-month mice with and without liver tumors. Mice with hepatic tumors showed 12,822 (1.8%) probes with differential methylation as compared to non-tumor animals, of which 8,656 (67.5%) were hypomethylated. We observed a significant enrichment of differential methylation in Gene Ontology (GO) terms and biological processes related to morphogenesis and development, and epigenomic alteration. Pathway enrichment revealed a predominance of hypermethylated neuronal signaling pathways linked to energy regulation and metabolic function, supporting metabolic consequences in the liver via BPA-induced disruption of neuronal signaling pathways. Hypothesis-driven pathway analysis revealed mouse and human genes linked to BPA exposure related to intracellular Jak/STAT and MAPK signaling pathways. Taken together, these findings are indicators of the relevance of the hepatic tumor phenotype seen in BPA-exposed mice to human health. This work demonstrates that epigenome-wide discovery experiments in animal models are effective tools for identification and understanding of paralagous epimutations salient to human disease.

John Wiley & Sons, Inc.

This article is protected by copyright. All rights reserved.

Accepted Article

Keywords

Hepatocellular carcinoma

Developmental Origins of Health and Disease (DOHaD)

Epigenetics

Environmental epigenetics

Bisphenol A (BPA)

Endocrine disruptors

Accepted Article

John Wiley & Sons, Inc.

This article is protected by copyright. All rights reserved.

Accepted Article

Introduction

Bisphenol A (BPA) is a high production volume monomer used in the manufacture of polycarbonate plastics and other consumer products that has been implicated as an endocrine disruptor, due to its ability to bind both canonical and non-canonical estrogen receptors (Welshons, et al., 2006). Biomonitoring studies routinely detect levels of BPA in urine in > 90% of adults in the United States, indicating that exposure to BPA is widespread (Calafat et al., 2008). Environmental BPA exposure is associated with several health outcomes in rodents and humans, including impaired fertility, altered immune and thyroid function, and increased risk for obesity, diabetes, and cardiovascular disease (Rochester, 2013). Furthermore, BPA has been implicated as a potential carcinogen when administered in early life, due to its association with proliferative tissue changes in rat mammary glands (Acevedo et al., 2013) and rat prostate glands (Ho et al., 2006) and with frank prostate cancer in mice with human prostate stem cell xenografts supplemented with sex steroid hormones to mimic human male aging (Prins et al., 2014).

Previously, we reported a dose-dependent increase in hepatic tumors, or combined incidence of hepatocellular carcinomas and hepatic adenomas, in 10-month mice perinatally exposed to one of three doses of BPA in the diet (Weinhouse et al., 2014). In contrast, no statistically significant relationship between liver tumors and BPA exposure in adult rodents was seen in the 1982 regulatory evaluation of BPA's carcinogenicity, which employed doses 200-20,000 times higher than those used in our study, supporting the importance of exposure timing (NTP 1982). The liver tumors we observed were evident at 10-months of age (Weinhouse et al., 2014), which represents early onset disease in mice, and the tumors did not exhibit the classical sexual dimorphism in incidence Male rodents and humans are two to four times as likely as females to present with hepatocellular carcinoma, a ratio that is largely accepted to result from

John Wiley & Sons, Inc.
This article is protected by copyright. All rights reserved.

the protective, anti-inflammatory effect of endogenous estrogen in females (Shi et al., 2014). We observed only a proliferative response in exposed animals with hepatic tumors, with no evidence of fibrosis or necrosis, indicating that cellular proliferation was likely a primary response to BPA, rather than a secondary, regenerative response to chemical-induced tissue injury (Weinhouse et al., 2014).

Studies of early life exposure to exogenous chemicals, including BPA, are increasingly focused on the epigenome as a potential mechanism for persistence of exposure effects across the life course (Singh and Li, 2012). The epigenome, or genome-wide collection of epigenetic marks that govern gene expression, may be particularly vulnerable to disruption during embryogenesis (Jirtle and Skinner, 2007). In addition, alterations that occur during this critical developmental window may persist into adulthood, influencing adult health outcomes (Jirtle and Skinner, 2007). Perinatal exposure to BPA has previously been shown to alter tail DNA methylation at the coat-color linked A^{vy} (viable yellow *Agouti*) metastable epiallele (Anderson et al., 2012a; Dolinoy et al., 2007) in weanling mice. Several other studies have identified epigenetic alterations at specific genes linked to BPA dose and tissue alterations (Avissar-Whiting et al., 2010; Greathouse et al., 2012; Weinhouse et al., 2015), supporting the hypothesis that epigenetic changes may mediate the relationship between early life BPA exposure and adult health outcomes. In particular, BPA exposure has been linked to epigenetic dysregulation of estrogen-associated target genes, including nuclear estrogen receptors in rats (Doshi et al., 2011) and developmental transcription factor Hoxa10 in mice and human mammary carcinoma cells (Bromer et al., 2010). Global epigenomic regulators are altered by BPA exposure, as well, including histone methyltransferase *Ezh2* (Doherty et al., 2010), maintenance DNA

John Wiley & Sons, Inc.
This article is protected by copyright. All rights reserved.

Accepted Article

methyltransferases *Dnmt3a* and *Dnmt3b* (Doshi, Mehta, Dighe, Balasinor, & Vanage, 2011) and methyl binding proteins *Mbd2* and *Mbd4* (Tang et al., 2012).

To date, few studies have investigated alterations to epigenetic marks across the genome following perinatal BPA exposure. Dhimolea et al. observed epigenome-wide alterations in DNA methylation in mammary tissue of 21-day-old Wistar-Furth rats exposed from gestational day 9 to postnatal day 1 to 250 µg BPA/kg BW/day via subcutaneous osmotic pumps, although the majority of transcriptional changes did not occur until postnatal day 50 (2014). We reported dose-dependent regions of altered methylation in CpG island shores in liver tissue of wild-type (*a/a*) offspring of A^{vy} mice heterogeneous for the A^{vy} allele exposed perinatally to 50 µg or 50 mg BPA/kg maternal diet, and noted alterations in pathways associated with metabolism and stimulus response (Kim et al., 2014). However, to our knowledge, no study to date has utilized an epigenome-wide platform to assess pathway level changes associated with both BPA exposure and the presence of an adverse health effect later in life in rodents or humans. Here, we use an epigenome-wide tiling array platform, which together with gene set analysis, identified neuronal signaling and metabolism as *de novo* pathways linked to BPA exposure and hepatic tumorigenesis in mice. Additionally, we provide evidence supporting our *a priori* hypothesis that specific inflammatory signaling pathways would be linked to murine exposure and disease. By mining human data curated in the Comparative Toxicogenomics Database, we deduce that BPA exposure has been linked to both neuronal and inflammatory signaling pathways described here, supporting the human health relevance of our experiments. The results provide a mechanistic hypothesis for how DNA methylation mediates the dose-dependent increase in hepatic tumors observed after perinatal BPA exposure.

Materials and Methods

John Wiley & Sons, Inc.
This article is protected by copyright. All rights reserved.

Accepted Article

Mouse Liver Samples

Mice were obtained from a colony generated by backcrossing C3H/HeJ mice carrying the viable yellow *Agouti* (A^{vy}) allele with C57BL/6J mice, followed by >200 generations of sibling mating (Waterland & Jirtle, 2003). The A^{vy} strain is isogenic (Waterland & Jirtle, 2003) and has been empirically confirmed to be genetically 93% C57BL/6J (Weinhouse et al., 2014). As previously described (Anderson et al 2012b), virgin *a/a* dams, 6 weeks of age, were randomly assigned to one of four phytoestrogen-free AIN-93G diets (diet 95092 with 7% corn oil substituted for 7% soybean oil; Harlan Teklad, Madison, WI): (1) standard diet; (2) standard diet supplemented with 50 ng BPA/kg diet; (3) standard diet supplemented with 50 µg BPA/kg diet; (*4*) standard diet supplemented with 50 mg BPA/kg diet. All diet ingredients were supplied by Harlan Teklad except BPA, which was supplied by NTP (National Toxicology Program, Durham NC). Following 2 weeks on their respective diets, at 8 weeks of age *a/a* virgin dams were mated with A^{vy}/a males, 7–8 weeks of age. All animals were housed in polycarbonate-free cages and provided *ad libitum* access to diet and BPA-free water. The dams remained on the assigned diets throughout pregnancy and lactation. This mating scheme produced approximately 50% wild-type (*a/a*) offspring and 50% heterozygous (A^{vy}/a) offspring.

The majority of A^{vy}/a mice were euthanized on post-natal day (PND) 22 (Anderson et al., 2012b). A subset of wild-type (*a/a*) mice (approximately 1 male and 1 female per litter for each BPA diet group) were then housed with a same-sex A^{vy}/a sibling and fed the standard phytoestrogen-free control diet until they were euthanized at 10 months of age, as described by Anderson et al. (Anderson et al., 2013). During dissection, liver tissue was collected and flash frozen in liquid nitrogen, followed by evaluation for histopathologic lesions, including benign and malignant tumors, as previously described (Weinhouse et al., 2014). Liver tissue

John Wiley & Sons, Inc.
This article is protected by copyright. All rights reserved.

measurements for free and conjugated (glucuronidated and sulfated) BPA in PND22 mouse liver samples (Anderson et al., 2012a) have confirmed liver BPA levels within the range of reported human environmental exposures (Vandenberg et al., 2012).

In this study, we combined offspring in the 50 ng and 50 µg BPA dose groups into one "low BPA" group for comparison with offspring in the 50 mg BPA, or "high BPA" group (n=16 offspring; n=4 male and n=4 female offspring exposed to "low BPA," or 50 ng or 50 µg BPA/kg maternal diet; n=4 male and n=4 female offspring exposed to "high BPA," or 50 mg BPA/kg maternal diet), as well as with wild-type *a/a* control mice (n=6 offspring; n=3 male and n=3 female).We chose to combine offspring in the two lower dose groups for two reasons. First, the lower two dose groups combined presented with approximately the same number of tumors as the high dose group alone. An analysis that separated the animals into three dose groups would likely have been underpowered to detect meaningful differential methylation, due to small numbers of tumors in low dose groups. Second, this choice was biologically sound, as we have reported previously that internal liver tissue BPA levels from animals exposed to the two lower doses were very similar, but that liver tissue levels from animals exposed to the high BPA dose were 100-fold higher than the low dose groups (Anderson et al., 2012.)

DNA Isolation

Total genomic DNA was isolated from 10-month liver tissue (n=22) using a standard phenol-chloroform extraction method. Briefly, approximately 10-15 mg of liver tissue was homogenized for three 20-second pulses at 15 Hz (TissueLyser, Qiagen) in 540 µl of lysis buffer (buffer ATL, Qiagen) and incubated overnight at 50 ºC with 60 µl Proteinase K. Lysate was then incubated with 12 µl RNase A for 10 minutes at 37 ºC. The DNA-containing aqueous phase was extracted twice with 600 µl phenol-chloroform-isoamyl alcohol, followed by a single extraction

John Wiley & Sons, Inc.
This article is protected by copyright. All rights reserved.

Accepted Article

with 600 µl chloroform, using Phase Gel Lock tubes (5 Prime, Gaithersburg, Maryland). 50 µl 3M sodium acetate was added to decanted aqueous phase. DNA was precipitated once with 1 mL of 100% ethanol and twice with 1 mL of 75% ethanol. Pellets were air dried and resuspended in 50 µl Tris-EDTA buffer during 2-hour incubation at 60 ºC with frequent mixing.

DNA Fragmentation

Genomic DNA was sheared to fragment sizes ranging from 200 to 1000 bp using manufacturer's instructions on an Episonic 1100 series sonicator (Farmingdale, NY). Briefly, 17 µg of DNA was divided into two volumes of 8.5 µg in separate PCR tubes and was sonicated in a polycarbonate plastic tube rack with a total process time of 15 minutes (15 second on and 30 second off cycles, amplitude of 18) in 8-20 ºC water. Water was monitored and cooled with sonicator cooling system every 5 minutes of process time. Fragment sizes for each sample were confirmed with ~1 µg DNA via gel electrophoresis. One sonicated aliquot per sample was enriched for methylated DNA, as described below. Matching sample aliquots were reserved as genomic input for co-hybridization with enriched fractions to microarrays.

Enrichment and Whole Genome Amplification of Methylated DNA

Methylated DNA fragments from one sonication aliquot per sample were enriched for methylcytosine using methyl-CpG binding domain-based capture (MBD-Cap) with the EpiMark Methylated DNA Enrichment Kit (New England BioLabs, Ipswich, Massachusetts). The EpiMark kit uses a fusion protein (MBD-Fc) containing the highly conserved methyl binding domain (MBD) of human MBD2 protein fused to the Fc tail of human IgG. MBD-Fc proteins and paramagnetic protein A beads were incubated for 15 minutes at room temperature, allowing Fc domains to couple with protein A beads, and washed twice with wash buffer. Fragmented genomic DNA was added to MBD-Fc/bead mixture, rotated at room temperature for 20 minutes,

John Wiley & Sons, Inc.
This article is protected by copyright. All rights reserved.

Accepted Article

and washed three times with wash buffer to discard unbound DNA. Captured methylated DNA was eluted with 100 µl of DNase-free water during a 15-minute incubation at 65 ºC. Residual unmethylated DNA fractions were reserved for downstream enrichment testing via qPCR. In order to obtain sufficient DNA for microarray hybridization, 10 ng of captured methylated DNA was amplified using GenomePlex Complete Whole Genome Amplification Kit (Sigma-Aldrich, St. Louis, Missouri).

Methylated DNA Enrichment Quality Assessment

Quality assessment for methylated DNA enrichment was performed via qPCR of two methylated regions at *Xist* and *H19* loci used as positive control probes on the microarray platform used in this study. Chromosomal coordinates of control probes were obtained directly from microarray manufacturers (Roche NimbleGen Inc., Madison, Wisconsin), and qPCR assays were designed to capture *Xist* and *H19* positive control probe sequences. Approximately 60 ng each of genomic input sonicated DNA (diluted 1:10), unmethylated DNA from uncaptured fraction reserved after enrichment step (diluted 1:10), and WGA enriched DNA (diluted 1:100) was analyzed for relative enrichment of fragments containing control probe sequences. Quantitative PCR was performed in duplicate 25 µl reactions using SYBR Green Master Mix (Qiagen Inc., Valencia, California), 0.25 pmol forward and reverse primers, and 60 ng input DNA from above, under the following reaction conditions: 95 ºC for 3 minutes, followed by 39 cycles of 10 seconds at 95 ºC, 62 ºC for 30 seconds, 72 ºC for 10 seconds, with a final incremental temperature decrease from 95 ºC for melt curve analysis to confirm product uniqueness. The average threshold cycle (*C(t)*) from duplicate reactions was calculated using CFX Manager Version1.6 software (Bio-Rad). A minimum of 10-fold enrichment of positive

John Wiley & Sons, Inc.
This article is protected by copyright. All rights reserved.

Accepted Article

control regions in methylated fraction over genomic fraction was confirmed for each sample prior to sample hybridization to microarrays.

Hybridization and Array Scanning

Experimental enriched and genomic input fractions for each sample were labeled with Cy5 and Cy3, respectively, with NimbleGen Dual-Color Labeling Kit (Roche NimbleGen, Madison, Wisconsin) following instructions in the NimbleGen Array User Guide (Nimblegen Array User Guide *DNA Methylation Arrays*, Version 7.2). Labeled fractions were pooled and co-hybridized to Roche NimbleGen Mouse DNA Methylation 3x720K CpG Island Plus RefSeq Promoter Arrays for 16-20 hours. These promoter DNA methylation tiling arrays contain three subarrays, each containing 720,000 probes that scan 15,980 CpG islands in 20,404 murine gene promoters. Probe tiling ranges from 2,960 bp upstream to 740 bp downstream of transcription start sites. Probes range in length from 50-75 bp with median probe spacing of 100 bp. Following hybridization, arrays were washed and scanned using a 2 μm resolution NimbleGen MS 200 Microarray Scanner (Dr. Thomas Glover, Department of Human Genetics, University of Michigan). All arrays were run by a single individual in two batches during January and March, months in which humidity and ozone levels were fairly consistently low.

Bioinformatics Pipeline

Array images were uploaded to NimbleGen DEVA software (version 2.3) and aligned using an automated alignment grid function. Raw signal intensities for each channel were exported using the software report function. Raw intensity values were background corrected using the *norm+exp-offset* method (to prevent loss of data that is common using background subtraction) and then quantile normalized across all samples. Quantile normalization was performed on untransformed intensity values. Following normalization, M values, or $\log_2$ ratios

John Wiley & Sons, Inc.
This article is protected by copyright. All rights reserved.

Accepted Article

of enriched sample signal intensity to input sample signal intensity, were computed for each feature on the array. Differentially enriched regions between dose and tumor groups were identified by comparing M values for each probe. Regression models testing for differential methylation in gene promoters across the epigenome were run for four pair-wise comparisons: 1) animals with tumors (n=16; n=8 males and n=8 females) versus animals without tumors (n=6; n=3 males and n=3 females); 2) animals exposed to low BPA (n=8; n=4 males and n=4 females) versus control animals (n=6; n=3 males and n=3 females); 3) animals exposed to high BPA (n=8; n=4 males and n=4 females) versus control animals; and 4) animals exposed to high BPA versus low BPA. In this analysis, all animals exposed to BPA also presented with hepatic tumors; therefore, the tumor versus non-tumor comparison is equivalent to the low and high BPA groups together compared to the control group. The three pair-wise dose group comparisons were tested using binary dose variables (low BPA vs. control; high BPA vs. control; high BPA vs. low BPA), adjusting for sex and tumor status. The additional pair-wise comparison of tumor vs. non-tumor samples was tested, adjusting for sex and dose. Linear regression models were fit using the lmFit function in the *limma* package in R. Standard errors were moderated with an empirical Bayes model using the eBayes function in *limma*. The False Discovery Rate (FDR) was computed for multiple comparison testing using the Benjamini-Hochberg correction of the initial p-values. Array features were annotated using the mm9 genome assembly. Probes were analyzed individually, rather than aggregated into larger windows or collapsed by gene promoter, in order to retain high resolution of the tiling array platform and to detect region-specific changes that may be masked by analysis of larger, smoothed windows. All analyses were performed in R version 3.1.1 using R packages *Ringo* and *limma*. Array probes were considered differentially enriched at $p<0.01$ (**Table 1**).

John Wiley & Sons, Inc.
This article is protected by copyright. All rights reserved.

Accepted Article

Validation of Top Differentially Methylated Probes

Quantitative DNA methylation patterns were analyzed via sodium bisulfite treatment followed by sequencing using Sequenom EpiTYPER MassARRAY technology in 5' gene promoter regions containing differentially methylated probes with the lowest p-values (top hits) for each of four analysis comparisons (β = ratio of enriched to input signal): *Lce1m* (tumor vs. non-tumor; β=0.641, p=7.11E-6), *Shmt2* (high BPA vs. low BPA; β=3.162, p=2.22E-7), *Foxp2* (low BPA vs. control; β=0.383, p=4.6E-6), and *Ift46* (high BPA vs. control; β=3.181, p=2.17E-5). Sodium bisulfite treatment was performed using the QIAGEN EpiTect Bisulfite Kit (QIAGEN) with approximately 1 µg input genomic DNA. EpiTYPER assays were designed using the Sequenom EpiDesigner tool (www.epidesigner.com), and top hit gene primer sets were assessed for unique products in the bisulfite-converted mouse and human genomes using the BiSearch ePCR tool (http://bisearch.enzim.hu). PCR was carried out in 25 µl reactions using approximately 50 ng of bisulfite-converted DNA, HotStarTaq master mix (QIAGEN Inc., Valencia, CA) and forward and reverse (0.1 pmol each) primers under the following conditions: 15 minutes at 95ºC, 40 cycles of (30 seconds at 94ºC, 30 seconds at annealing temperature (T_A), 1 minute at 72ºC), 10 minutes at 72ºC. The third most significant probe in the tumor vs. non-tumor comparison was chosen for validation, because the first two did not contain CpG sites and were not within CpG islands, with adjacent regions of high CpG density. This DNA microarray includes some probe sequences that do not contain CpG sites but are located adjacent to CpG sitse; therefore, DNA fragments that contain methylated CpG sites adjacent to these probe sequences may be enriched during MBD-cap and identified as "differentially methylated." Primer sequences for bisulfite sequencing of microarray top hits are listed in **Table 2**.

John Wiley & Sons, Inc.
This article is protected by copyright. All rights reserved.

Accepted Article

Dose- and tumor-dependent DNA methylation changes in 10-month mice with tumors, as compared to 10-month control mice without tumors, were assessed using repeated measures mixed models (PROC MIXED), with individual CpG sites defined as repeated measures, in order to account for lack of independence of multiple CpG sites at a single locus within an individual animal (**Table 3**). One model was run per candidate gene, including four predictors: repeated CpG site, dichotomous tumor, dichotomous sex, and ordinal dose. Fixed effects of the dependent variable assessed associations between dose and tumor status with average methylation at a locus. Dose was coded as an ordinal variable for all administered doses (control=0, 50 ng BPA/kg maternal diet=1, 50 µg BPA/kg maternal diet=2, and 50 mg BPA/kg maternal diet=3). In order to directly validate microarray results, three contrast statements were included to closely mimic the comparisons in the regression models run on the microarray data ("low BPA," or an average of effects of the two lowest doses, as compared to control; "high BPA," or the highest dose, as compared to control, and "high BPA," or the highest dose, as compared to "low BPA", or an average of the effects of the two lowest doses). The tumor vs. non-tumor comparison was directly tested with a dichotomous tumor variable. All models contained a random intercept to cluster data by litter. In the model testing DNA methylation at *Ift46* (4 CpG sites in the assay), an unstructured variance-covariance matrix was computed from the data (option *type=un*), in agreement with prior studies indicating site-specific basal methylation and lability. In models testing DNA methylation at *Foxp2*, *Shmt2*, and *Lce1m*, loci with large numbers of CpG sites, an unstructured variance-covariance matrix could not be computed and empirical standard errors were instead calculated (option *empirical*). All statistical analyses were performed in SAS v9.4 (Cary, NC).

Pathway and GO Term Enrichment Analysis

John Wiley & Sons, Inc.
This article is protected by copyright. All rights reserved.

Accepted Article

Complete probe lists with p-values and β values (normalized ratios of enriched to input signal intensities) for each of four comparisons were uploaded to the LRpath web tool for pathway (BioCarta, KEGG, Panther, EHMN, and pFAM) and GO term (GO Biological Processes, GO Molecular Function, and GO Cellular Component) enrichment analyses. LRpath tests for gene sets with significantly higher significance values than expected at random using logistic regression, allowing data to remain on a continuous scale (Sartor et al., 2009).

GO terms (**Table 4**) and pathway terms (**Table 5**) with FDR values <0.1 were first assessed for evidence of statistically significant changes in pathways or cellular processes linked to BPA exposure and HCC. A hypothesis-driven approach investigating the influence of Jak/Stat and Mapk signaling pathways was pursued, as well. First, all pathways related to Jak/Stat and Mapk signaling with p-values <0.05 in each of the above-mentioned four comparisons were identified. Unique mouse gene IDs in the selected pathways that were reported by LRpath as significant (average p-value <0.05 across probes for each gene) and were related to Jak/Stat (70 mouse gene IDs) and Mapk (110 mouse gene IDs) across all four dose comparisons were annotated with gene names and descriptions using NCBI's Batch Entrez tool (http://www.ncbi.nlm.nih.gov/sites/batchentrez). To assess the relevance of these results to the human pathway response to BPA exposure, genes within human JAK/STAT (61 human gene IDs) and MAPK (177 human gene IDs) signaling pathways known to be altered by BPA were downloaded from The Comparative Toxicogenomics Database (CTD; http://ctdbase.org/) and compared to the mouse gene IDs. The gene overlaps in these pathways are listed in **Supplementary Tables S3** and **S4** and shown visually in **Figures 1** and **2**. Gene set overlaps were overlaid onto KEGG pathways using the KEGG Pathway Mapper tool (http://www.genome.jp/kegg/pathway.html).

John Wiley & Sons, Inc.
This article is protected by copyright. All rights reserved.

Accepted Article

Accepted Article

Results

Of the four comparisons, the largest number of changes were observed for tumor vs. non-tumor animals (12,822 probes with $p<0.01$), followed by high BPA vs. control, high BPA vs. low BPA, and, with the fewest probes, low BPA vs. control (**Table 1).** In most comparisons, roughly two-thirds of differentially methylated probes were hypomethylated and one-third were hypermethylated, with the exception of the high BPA vs. low BPA comparison, in which the pattern was reversed (**Table 1**).

Validation of Top Differentially Methylated Probes

Technical validation of the microarray platform used in this study was performed via bisulfite sequencing of 5' gene promoter regions containing differentially methylated probes with the lowest p-values (top hits) for each of four analysis comparisons (**Tables 2 and 3.)** *Foxp2*, *Ift46*, and *Shmt2* displayed differential methylation ($p<0.05$) on bisulfite sequencing in at least one of four comparisons (**Table 3**). However, differential methylation on microarray was not consistently observed in the same tumor or dose comparison in bisulfite sequencing results (**Table 3**). These results indicate that microarray data are valid and meaningful, but that results should be interpreted broadly across comparisons tested.

Gene Ontology Term Enrichment

Since few individual probes displayed significant altered methylation by dose group or tumor status following FDR correction for multiple testing, we opted to test for groups of genes significantly enriched with differential methylation using Gene Ontology (GO), which can greatly increase the power to detect significant changes or trends (Ashburner et al., 2000). Thirty-three GO terms were enriched with differential methylation for animals with tumors versus without tumors (FDR<0.1) **(Table 4a, full significant gene lists in Supplemental Table**

John Wiley & Sons, Inc.
This article is protected by copyright. All rights reserved.

S1). Genes in all 33 of the significant biological processes were hypermethylated, except two: *positive regulation of cell matrix adhesion* (p=5.1E-5, FDR=0.05) and *regulation of the force of heart contraction* (p=0.00072, FDR=0.064). The majority of these terms (n=27) were involved in morphogenesis or development (including *hepaticobiliary system development,* p=1.0E-5, FDR=0.0035; and *organ morphogenesis,* p=4.0E-4, FDR=0.05). The most significant GO term was *middle ear morphogenesis,* which contained 5 genes (out of 11) with a change in methylation and demonstrated a hypermethylation pattern (p=1.9E-8, FDR=4.6E-5). These five genes appeared 10 or 11 times each associated with the 33 GO terms on this list, indicating a high degree of overlap in these processes. Six GO terms related to epigenomic alteration displayed promoter hypermethylation in this comparison (*demethylation*, p=0.00019, FDR=0.03; *histone modification*, p=2.9E-4, FDR=0.040; *covalent chromatin modification*, p=2.46E-4, FDR=0.04; *positive regulation of DNA repair*, p=3.7E-4, FDR=0.05; and *one-carbon metabolic process,* p=0.0017, FDR=0.11). *Demethylation* contained eight genes, including CYP450 enzymes *Cyp3a11*, *Cyp3a16*, *Cyp3a44*, and three lysine-specific demethylases. *One-carbon metabolic process* contained 31 genes, including mitochondrial *serine hydroxymethyltransferase 2* (*Shmt2*) and *methionine adenosyltransferase I α* (*Mat1a*), which catalyzes the biosynthesis of methyl donor S-adenosylmethionine (Rountree et al., 2008).

Four GO terms were significant in the low BPA vs. control comparison (**Table 4b, full significant gene lists in Supplemental Table S1**). Three terms that refer primarily to cellular transport were hypermethylated, including *Golgi to plasma membrane transport* (p=1.2E-5, FDR=0.03); *macromolecule transmembrane transporter activity* (p=1.4E-4, FDR=0.04); and *protein transmembrane transporter activity* (p=1.4E-4, FDR=0.04). The remaining term, *NADP*

John Wiley & Sons, Inc.
This article is protected by copyright. All rights reserved.

Accepted Article

or NADPH binding (p=5.3E-4, FDR=0.099), was hypomethylated, and may be broadly related to the redox state of the cells investigated.

The high BPA vs. control comparison showed seven significant GO terms (**Table 4b, full significant gene lists in Supplemental Table S1**), including two terms related to transcription factor binding to DNA (*sequence specific DNA binding*, p=1.5E-4, FDR=0.04; *sequence specific DNA binding transcription factor activity*, p=2.6E-4, FDR=0.05) and two related to activity of ligases that form carbon-sulfur bonds (*acid-thiol ligase activity*, p=5.1E-5, FDR=0.03, *ligase activity, forming carbon-sulfur bonds*, p=4.02E-4, FDR=0.06). The remaining three terms refer to membrane-bound proteins (*extrinsic to membrane*, p=3.15E-5, FDR=0.0061; *heterotrimeric G-protein complex*, p=3.27E-5, FDR=0.006; *extrinsic to plasma membrane,* p=3.2E-4, FDR=0.04). The remaining comparison, high BPA vs. low BPA, showed the same seven significant GO terms listed above for the high BPA vs. control comparison (**Table 4b, full significant gene lists in Supplemental Table S1**).

Pathway Enrichment

Testing for pathways enriched with differential methylation revealed a predominance of hypermethylated neuronal signaling pathways in the high BPA vs. control comparison, including histamine H1 and H2 receptor mediated signaling, 5HT1 and 5HT4 serotonin receptor mediated signaling pathways, β_1, β_2, and β_3 adrenergic receptor signaling pathways, thyrotropin-releasing hormone receptor signaling, GABA and glutamate receptor signaling, and muscarinic acetylcholine receptor 1, 2, 3 and 4 signaling (**Table 5, full significant gene lists in Supplemental Table S2**). Non-neuronal pathways significant in the high BPA vs. control comparison include Erk signaling (*role of Erk5 in neuronal survival*, p=1.8E-4, FDR=0.03) and PI3K signaling (*PI3 kinase pathway*, p=0.010, FDR=0.05) pathways (**Table 5, full significant**

John Wiley & Sons, Inc.
This article is protected by copyright. All rights reserved.

Accepted Article

gene lists in Supplemental Table S2). Two pathway terms were significant in the low BPA vs. control comparison, including *selenocompound metabolism* (p=1.3E-5, FDR=0.003), which may be linked to cellular redox state (**Table 5, full significant gene lists in Supplemental Table S2**).

In addition to our agnostic assessment of altered biological pathways, we further analyzed the data using a hypothesis-driven approach for relevance to human exposure to BPA and to the HCC phenotype under study. We hypothesized that Jak/Stat and Mapk signaling pathways would be altered in a tumor status- and dose-dependent manner. Jak/Stat and Mapk signaling have previously been implicated in the literature in mediating estrogen-dependent protection of females from hepatocellular carcinoma (Sekine et al., 2004, Shi et al., 2014a). Hypothesis-driven analysis (see methods for details) revealed 70 differentially methylated mouse genes in the selected concepts related to Jak/Stat and 110 differentially methylated genes related to Mapk across all four dose comparisons. Sixty-one genes within the human JAK/STAT pathways and 177 genes within human MAPK signaling pathways with prior evidence of response to BPA were compared to the 70 and 110 mouse gene lists. Mouse microarray results overlapped with human homologs with known interactions with BPA at 10 genes in JAK/STAT signaling (**Figure 1, Supplemental Table S3**), including the kinase *JAK1* and the transcription factors *STAT5A* and *STAT5B*, and at 32 genes in MAPK signaling (**Figure 2, Supplemental Table S4),** including the oncogene *MYC* and ten members of the *mitogen-activated kinase* (*MAP kinase*) family.

Discussion

In the present study, we used epigenome-wide microarrays to detect differential DNA methylation in 5' gene promoters in liver tumor tissue of 10-month-old isogenic mice that were transiently exposed to BPA during gestation and lactation. Although we did not identify many

John Wiley & Sons, Inc.
This article is protected by copyright. All rights reserved.

Accepted Article

individual probes with FDR<0.1, gene set enrichment testing detected subtle but consistent changes across GO terms and pathways. Furthermore, these data indicate patterns of change that suggest specific biological responses and provide direction for future work.

We identified several processes with altered epigenetic patterning across the genome, supporting the hypothesis of large scale, yet subtle, epigenomic change in mice following BPA exposure. Animals with liver tumors showed enrichment for genes in one-carbon metabolic process as compared to animals without liver tumors. This GO term included mitochondrial *serine hydroxymethyltransferase 2* (*Shmt2*) and *methionine adenosyltransferase I α* (*Mat1a*), which are linked not only to regulation of epigenetic patterning but also to liver function and pathology (Liu et al., 2007; Rountree et al., 2008). Morphogenic and developmental processes, which were hypermethylated in mice with tumors as compared to mice without tumors, may be altered due to cancer-related pathway reversion to embryonic states (Hanahan and Weinberg, 2011) or to a relative increase in the proportion of stem cells in liver tissue, suggested by a dose-dependent increase in oval cell hyperplasia noted in mice with hepatic tumors (Weinhouse et al., 2014).

Agnostic pathway analysis revealed a predominance of hypermethylated neuronal pathways linked to energy regulation and metabolic function, suggesting that BPA-induced disruption of neuronal signaling pathways may have metabolic consequences in the liver. Histamine receptor signaling plays a role in the development of hyperlipidemia-induced non-alcoholic steatohepatitis (NASH) (Wang et al., 2010). Histamine (Knigge et al., 1984) and serotonin (Castrogiovanni et al., 2014) also regulate growth hormone secretion and IGF-1 production. β-adrenergic receptor signaling has been reported to drive lipolysis in adipose tissue (Thompson et al., 2014), suggesting that pathway suppression is consistent with steatosis

John Wiley & Sons, Inc.
This article is protected by copyright. All rights reserved.

Accepted Article

previously reported in study animals (Weinhouse et al., 2014). Metabolic dysfunction has been associated with both exposure to environmental estrogens and liver disease states. Elevated IGF-1 is a risk factor for HCC development, possibly due to altered metabolism secondary to liver damage (Lukanova et al., 2014). Type II diabetes confers a 2.3 fold increase in risk for HCC, regardless of other risk factors, including cirrhosis (Lukanova et al., 2014). Some hormonal contraceptives have been linked to altered metabolism, as well. Depot medroxyprogesterone acetate increased glucose and insulin levels in the first 18-30 months of use (Berenson et al., 2011), and African-American women using oral contraceptives were more insulin resistant than controls (Frempong et al., 2008). This may be relevant, because hepatic adenomas (HA), a rare form of benign liver tumor historically associated nearly exclusively with long term use of high dose oral contraceptives, have been increasingly linked to hormonal or metabolic imbalances that stimulate hepatocyte proliferation (Farges & Dokmak, 2010; González-Lara, et al., 2013).

Suppression of neuronal pathways as suggested by the observed promoter DNA hypermethylation response may allow for higher tissue levels of Igf1 and increased proliferative response in the liver. However, these results should be interpreted with caution, as none of the 19 pathway terms related to IGF signaling, insulin signaling, or growth hormone signaling were statistically enriched for in these analyses. In addition, neuronal signaling pathways identified here may be related to phenotypic effects of BPA exposure other than liver tumors. Perinatal BPA exposure has been linked to hyperactivity and anxiety (Anderson et al., 2013) as well as decreased hippocampal serotonin signaling (Texel et al., 2012).

In addition to our agnostic results, we took a hypothesis-driven approach. The classical sexual dimorphism in incidence not seen in our study is well accepted to result from a suppression of IL-6 production by endogenous estradiol and downstream suppression of STAT3

John Wiley & Sons, Inc.
This article is protected by copyright. All rights reserved.

Accepted Article

signaling (Sekine et al., 2004). As Jak/Stat and Mapk signaling pathways have previously been implicated in male: female dimorphism in incidence, we investigated a potential link between these pathways and hepatic tumors in BPA-exposed mice. We report an overlap of genes implicated in Jak/STAT and MAPK signaling with altered 5' promoter methylation in mice perinatally exposed to BPA presenting with hepatic tumors, with genes linked to the same pathways noted to respond to human BPA exposure in The Comparative Toxicogenomics Database (Davis et al., 2014). Three key overlapping genes, *Jak1*, *Stat5b*, and *Akt1*, have previously characterized roles linked to liver carcinogenesis. JAK1 activation mediates PI3K and Akt phosphorylation and contributes to downstream inflammation in immortalized human HSC (LX-2) cells and in human HCC (HepG2) cells (Niu et al., 2007). STAT5b activation is associated with epithelial-to-mesenchymal transition in human clinical HCC samples, and is linked to younger age of onset and advanced tumor stages (Lee et al., 2006). STAT5b is also required for sexually dimorphic liver gene expression (Udy et al., 1997).

In summary, these results indicate that BPA may lead to liver carcinogenesis and metabolic dysfunction via alterations in neuronal signaling pathways. In addition, our results identified specific genes within Jak/Stat and Mapk signaling pathways that may mediate the link between early life BPA exposure and later life hepatic tumors in mice. We compared differentially methylated gene lists from our rodent BPA study with prior data on genes associated with human BPA exposure, rather than with hepatic tumors. This approach allowed us to distinguish genes that are potential early causal factors in tumorigenesis linked to BPA exposure from genes associated with the highly dysregulated biology of tumor tissue that might be common to many tumors unrelated to BPA exposure. However, these data must be interpreted in the context of limitations of experimental design. First, DNA samples for

John Wiley & Sons, Inc.
This article is protected by copyright. All rights reserved.

Accepted Article

microarray experiments were extracted from liver tumor tissue. Epithelial liver tumors are primarily composed of hepatocytes, but may also contain vascular, nervous, and fat tissue. Thus, we cannot rule out that differences in percent DNA methylation may be due wholly or in part to differences in relative proportions of cell types within tissue samples. Second, further experiments are needed to fully characterize how identified pathways act in the context of our observed liver tumor phenotype. Future studies that include observation of animals at earlier time points prior to tumor development would clarify temporality of inflammation and its potential link with perinatal BPA exposure. Third, in this study, we did not test whether expression of identified genes was regulated by DNA methylation. Experimental assessment of a regulatory role for DNA methylation in expression change is complicated by several factors. DNA methylation may be temporally unlinked from expression change; that is, DNA methylation changes may represent markers of concurrent expression change, but they may also represent residual markers of prior expression change or markers of expression change "risk", or priming for a future response. Therefore, a large number of experimental time points would be required to fully test this question. In addition, in order to assess a causal regulatory role for DNA methylation changes, experimental tools for inducing targeted and precise DNA methylation change would be required. These tools are under development but are not yet widely or easily available, nor do they provide unambiguous answers.

Author Contributions

CW completed microarray experiments, analysed data, and wrote the manuscript. OSA generated the liver samples and assisted with sample preparation. MAS and CF provided substantive

John Wiley & Sons, Inc.
This article is protected by copyright. All rights reserved.

Accepted Article

bioinformatics advice and assistance with data analysis. KES assisted with data analysis. DCD, CH, and MAS oversaw the study and provided comments on the manuscript.

Acknowledgements

The authors thank Dr. Thomas Glover and Sountharia Rajendran for training and equipment assistance with microarray experiments.

Funding Information

This work was supported by a pilot grant from the Michigan Nutrition Research Obesity Center, MNORC (P30 DK089503), as well as NIH grant R01 ES017524 and the University of Michigan NIEHS Center for Lifestage Environmental Exposures and Disease (M-LEEaD; P30 ES017885). Support for CW was provided by NIEHS Institutional Training Grant T32 ES007062.

Accepted Article

References

Acevedo, N., Davis, B., Schaeberle, C. M., Sonnenschein, C., & Soto, A. M. (2013). Perinatally administered bisphenol a as a potential mammary gland carcinogen in rats. *Environmental Health Perspectives*, *121*(9).

Anderson, O. S., Nahar, M. S., Faulk, C., Jones, T. R., Liao, C., Kannan, K., … Dolinoy, D. C. (2012a). Epigenetic responses following maternal dietary exposure to physiologically relevant levels of bisphenol A. *Environmental and Molecular Mutagenesis*.

Anderson, O. S., Nahar, M. S., Faulk, C., Jones, T. R., Liao, C., Kannan, K., … Dolinoy, D. C. (2012b). Epigenetic responses following maternal dietary exposure to physiologically relevant levels of bisphenol A. *Environmental and Molecular Mutagenesis*.

Anderson, O. S., Peterson, K. E., Sanchez, B. N., Zhang, Z., Mancuso, P., & Dolinoy, D. C. (2013). Perinatal bisphenol A exposure promotes hyperactivity, lean body composition, and hormonal responses across the murine life course. *FASEB Journal : Official Publication of the Federation of American Societies for Experimental Biology*.

Ashburner, M., Ball, C. A., Blake, J. A., Botstein, D., Butler, H., Cherry, J. M., … Sherlock, G. (2000). Gene ontology: tool for the unification of biology. The Gene Ontology Consortium. *Nature Genetics*, *25*(1), 25–9.

John Wiley & Sons, Inc.

This article is protected by copyright. All rights reserved.

Avissar-Whiting, M., Veiga, K. R., Uhl, K. M., Maccani, M. A., Gagne, L. A., Moen, E. L., & Marsit, C. J. (2010). Bisphenol A exposure leads to specific microRNA alterations in placental cells. *Reproductive Toxicology (Elmsford, N.Y.)*, *29*(4), 401–6.

Baccarelli, A., & Bollati, V. (2009). Epigenetics and environmental chemicals. *Current Opinion in Pediatrics*, *21*(2), 243–51.

Berenson, A. B., van den Berg, P., Williams, K. J., & Rahman, M. (2011). Effect of injectable and oral contraceptives on glucose and insulin levels. *Obstetrics and Gynecology*, *117*(1), 41–7.

Calafat, A. M., Ye, X., Wong, L.-Y., Reidy, J. A., & Needham, L. L. (2008). Exposure of the U.S. population to bisphenol A and 4-tertiary-octylphenol: 2003-2004. *Environmental Health Perspectives*, *116*(1), 39–44.

Carcinogenesis Bioassay of Bisphenol A (CAS No. 80-05-7) in F344 Rats and B6C3F1 Mice (Feed Study). (1982). *National Toxicology Program Technical Report Series*, *215*, 1–116. 0

Castrogiovanni, P., Musumeci, G., Trovato, F. M., Avola, R., Magro, G., & Imbesi, R. (2014). Effects of high-tryptophan diet on pre- and postnatal development in rats: a morphological study. *European Journal of Nutrition*, *53*(1), 297–308.

Dhimolea, E., Wadia, P. R., Murray, T. J., Settles, M. L., Treitman, J. D., Sonnenschein, C., … Soto, A. M. (2014). Prenatal exposure to BPA alters the epigenome of the rat mammary gland and increases the propensity to neoplastic development. *PloS One*, *9*(7), e99800.

Doherty, L. F., Bromer, J. G., Zhou, Y., Aldad, T. S., & Taylor, H. S. (2010). In utero exposure to diethylstilbestrol (DES) or bisphenol-A (BPA) increases EZH2 expression in the mammary gland: an epigenetic mechanism linking endocrine disruptors to breast cancer. *Hormones & Cancer*, *1*(3), 146–55.

Dolinoy, D. C., Huang, D., & Jirtle, R. L. (2007). Maternal nutrient supplementation counteracts bisphenol A-induced DNA hypomethylation in early development. *Proceedings of the National Academy of Sciences of the United States of America*, *104*(32), 13056–61.

Dolinoy, D. C., & Jirtle, R. L. (2008). Environmental epigenomics in human health and disease. *Environmental and Molecular Mutagenesis*, *49*(1), 4–8.

Doshi, T., Mehta, S. S., Dighe, V., Balasinor, N., & Vanage, G. (2011). Hypermethylation of estrogen receptor promoter region in adult testis of rats exposed neonatally to bisphenol A. *Toxicology*, *289*(2-3), 74–82.

Farges, O., & Dokmak, S. (2010). Malignant transformation of liver adenoma: an analysis of the literature. *Digestive Surgery*, *27*(1), 32–8.

John Wiley & Sons, Inc.

This article is protected by copyright. All rights reserved.

Accepted Article

Frempong, B. A., Ricks, M., Sen, S., & Sumner, A. E. (2008). Effect of low-dose oral contraceptives on metabolic risk factors in African-American women. *The Journal of Clinical Endocrinology and Metabolism*, *93*(6), 2097–103.

González-Lara, M. F., Córdova-Ramón, J. C., Gamboa-Domínguez, A., Cosme-Labarthe, J., & Carrillo-Pérez, D. L. Hepatocellular carcinoma arising in a telangiectatic hepatocellular adenoma. *Annals of Hepatology*, *12*(4), 626–8.

Greathouse, K. L., Bredfeldt, T., Everitt, J. I., Lin, K., Berry, T., Kannan, K., … Walker, C. L. (2012). Environmental Estrogens Differentially Engage the Histone Methyltransferase EZH2 to Increase Risk of Uterine Tumorigenesis. *Molecular Cancer Research : MCR*, *10*(4), 546–57.

Hanahan, D., & Weinberg, R. A. (2011). Hallmarks of cancer: the next generation. *Cell*, *144*(5), 646–74.

Ho SM, Tang WY, Belmonte de Frausto J, Prins GS. (2006). Developmental exposure to estradiol and bisphenol A increases susceptibility to prostate carcinogenesis and epigenetically regulates phosphodiesterase type 4 variant 4. *Cancer Res*, 66(11): 5624-32.

Jirtle, R. L., & Skinner, M. K. (2007). Environmental epigenomics and disease susceptibility. *Nature Reviews. Genetics*, *8*(4), 253–62.

Kim, J. H., Sartor, M. A., Rozek, L. S., Faulk, C., Anderson, O. S., Jones, T. R., … Dolinoy, D. C. (2014). Perinatal bisphenol A exposure promotes dose-dependent alterations of the mouse methylome. *BMC Genomics*, *15*, 30.

Knigge, U., Thuesen, B., Wollesen, F., Dejgaard, A., & Christiansen, P. M. (1984). Histamine-induced paradoxical growth hormone response to thyrotropin-releasing hormone in normal men. *The Journal of Clinical Endocrinology and Metabolism*, *58*(4), 692–7.

Liu, S.-P., Li, Y.-S., Chen, Y.-J., Chiang, E.-P., Li, A. F.-Y., Lee, Y.-H., … Chen, Y.-M. A. (2007). Glycine N-methyltransferase-/- mice develop chronic hepatitis and glycogen storage disease in the liver. *Hepatology (Baltimore, Md.)*, *46*(5), 1413–25.

Lukanova, A., Becker, S., Hüsing, A., Schock, H., Fedirko, V., Trepo, E., … Kaaks, R. (2014). Prediagnostic plasma testosterone, sex hormone-binding globulin, IGF-I and hepatocellular carcinoma: etiological factors or risk markers? *International Journal of Cancer. Journal International Du Cancer*, *134*(1), 164–73.

Niu, L., Wang, X., Li, J., Huang, Y., Yang, Z., Chen, F., … Cao, Q. (2007). Leptin stimulates alpha1(I) collagen expression in human hepatic stellate cells via the phosphatidylinositol 3-kinase/Akt signalling pathway. *Liver International : Official Journal of the International Association for the Study of the Liver*, *27*(9), 1265–72.

Accepted Article

This article is protected by copyright. All rights reserved.

Prins, G. S., Hu, W.-Y., Shi, G.-B., Hu, D.-P., Majumdar, S., Li, G., … van Breemen, R. B. (2014). Bisphenol A promotes human prostate stem-progenitor cell self-renewal and increases in vivo carcinogenesis in human prostate epithelium. *Endocrinology*, *155*(3), 805–17.

Rochester, J. R. (2013). Bisphenol A and human health: a review of the literature. *Reproductive Toxicology (Elmsford, N.Y.)*, *42*, 132–55.

Rountree, C. B., Senadheera, S., Mato, J. M., Crooks, G. M., & Lu, S. C. (2008). Expansion of liver cancer stem cells during aging in methionine adenosyltransferase 1A-deficient mice. *Hepatology (Baltimore, Md.)*, *47*(4), 1288–97.

Sartor, M. A., Leikauf, G. D., & Medvedovic, M. (2009). LRpath: a logistic regression approach for identifying enriched biological groups in gene expression data. *Bioinformatics (Oxford, England)*, *25*(2), 211–7.

Shi, L., Feng, Y., Lin, H., Ma, R., & Cai, X. (2014). Role of estrogen in hepatocellular carcinoma: is inflammation the key? *Journal of Translational Medicine*, *12*(1), 93.

Singh, S., & Li, S. S.-L. (2012). Epigenetic effects of environmental chemicals bisphenol A and phthalates. *International Journal of Molecular Sciences*, *13*(8), 10143–53.

Tang, W., Morey, L. M., Cheung, Y. Y., Birch, L., Prins, G. S., & Ho, S. (2012). Neonatal exposure to estradiol/bisphenol A alters promoter methylation and expression of Nsbp1 and Hpcal1 genes and transcriptional programs of Dnmt3a/b and Mbd2/4 in the rat prostate gland throughout life. *Endocrinology*, *153*(1), 42–55.

Texel, S. J., Camandola, S., Ladenheim, B., Rothman, S. M., Mughal, M. R., Unger, E. L., … Mattson, M. P. (2012). Ceruloplasmin deficiency results in an anxiety phenotype involving deficits in hippocampal iron, serotonin, and BDNF. *Journal of Neurochemistry*, *120*(1), 125–34.

Thompson, N., Huber, K., Bedürftig, M., Hansen, K., Miles-Chan, J., & Breier, B. H. (2014). Metabolic programming of adipose tissue structure and function in male rat offspring by prenatal undernutrition. *Nutrition & Metabolism*, *11*(1), 50.

Udy, G. B., Towers, R. P., Snell, R. G., Wilkins, R. J., Park, S. H., Ram, P. A., … Davey, H. W. (1997). Requirement of STAT5b for sexual dimorphism of body growth rates and liver gene expression. *Proceedings of the National Academy of Sciences of the United States of America*, *94*(14), 7239–44.

Vandenberg, L. N., Chahoud, I., Heindel, J. J., Padmanabhan, V., Paumgartten, F. J. R., & Schoenfelder, G. (2012). Urinary, circulating, and tissue biomonitoring studies indicate widespread exposure to bisphenol A. *Ciência & Saúde Coletiva*, *17*(2), 407–34.

John Wiley & Sons, Inc.

This article is protected by copyright. All rights reserved.

Accepted Article

Wang, H., Li, J., Gao, Y., Xu, Y., Pan, Y., Tsuji, I., … Li, X.-M. (2010). Xeno-oestrogens and phyto-oestrogens are alternative ligands for the androgen receptor. *Asian Journal of Andrology*, *12*(4), 535–47.

Waterland, R. A., & Jirtle, R. L. (2003). Transposable elements: targets for early nutritional effects on epigenetic gene regulation. *Molecular and Cellular Biology*, *23*(15), 5293–300.

Weinhouse, C., Anderson, O. S., Bergin, I. L., Vandenbergh, D. J., Gyekis, J. P., Dingman, M. A., … Dolinoy, D. C. (2014). Dose-dependent incidence of hepatic tumors in adult mice following perinatal exposure to bisphenol A. *Environmental Health Perspectives*, *122*(5), 485–91.

Weinhouse C., Bergin I.L., Harris C., Dolinoy D.C. (2015) *Stat3* is a candidate epigenetic biomarker of perinatal bisphenol A exposure associated with murine hepatic tumors with implications for human health. Epigenetics. Epub ahead of print.

Welshons, W. V, Nagel, S. C., & vom Saal, F. S. (2006). Large effects from small exposures. III. Endocrine mechanisms mediating effects of bisphenol A at levels of human exposure. *Endocrinology*, *147*(6 Suppl), S56–69.

Accepted Article

John Wiley & Sons, Inc.

This article is protected by copyright. All rights reserved.

Accepted Article

Table 1. Microarray probes exhibiting differential methylation (p<0.01) by BPA dose and tumor status.

Comparison	**Total probes** *N (% of array probes)*	**Hypermethylated probes** *N (% of total differential probes)*	**Hypomethylated probes** *N (% of total differential probes)*
Tumor vs. non-tumor	12,822 (1.8)	4,166 (32.5)	8,656 (67.5)
High BPA vs. control	9,649 (1.3)	3,182 (33)	6,467 (67)
Low BPA vs. control	3,752 (0.52)	1,510 (40.2)	2,242 (59.8)
High BPA vs. low BPA	7,308 (1.0)	4,763 (65.2)	2,545 (34.8)

John Wiley & Sons, Inc.

This article is protected by copyright. All rights reserved.

Accepted Article

Table 2. Primer sets for bisulfite sequencing

Assay	Forward Primer	Reverse Primer	Product Size	T_A	#CpG sites
Lce1m	5'-TTAGATTGTTGATGGTTGTTGTTGT-3'	5'-AATACCCTCCAACCTCTTCCTACTA-3'	457 bp	57ºC	14
Shmt2	5'-TTGGGTGATTATAAGATTTTATTTAGG-3'	5'-AAAACTTTTCAAACAAAACTCTCCA-3'	484 bp	57ºC	16
Foxp2	5'-ATTTTGGGGATTGTTAAGAAGTAGT-3'	5'-CCCAACTTTTTCCAAAAATAAAAAA-3'	487 bp	54ºC	8
Ift46	5'-TGTTTTTGGGTTAGGAAATTTTTTT-3'	5'-TCTCATCTTCTCTTACCTTACTATCCTAAA-3'	236 bp	48ºC	4

John Wiley & Sons, Inc.

This article is protected by copyright. All rights reserved.

Accepted Article

Table 3. Microarray validation using bisulfite sequencing

	Microarray			Bisulfite sequencing validation		
Gene	Comparison	β coefficient*	*P*-value	Comparison	β coefficient**	*P*-value
Lce1m	Tumor vs. Non-tumor	0.64	7.10E-06	Tumor vs. Non-tumor	0.010	0.77
				Low vs. Control	0.018	0.85
				High vs. Control	0.024	0.64
				High vs. Low	0.0060	0.39
Foxp2	Low vs. Control	0.38	4.60E-06	Tumor vs. Non-tumor	-0.0089	0.015
				Low vs. Control	-0.0059	0.59
				High vs. Control	0.0074	0.081
				High vs. Low	0.013	0.14
Ift46	High vs. Control	3.2	2.20E-05	Tumor vs. Non-tumor	-0.0048	0.61
				Low vs. Control	0.027	0.018
				High vs. Control	0.010	0.075
				High vs. Low	-0.017	0.42
Shmt2	High vs. Low	3.2	2.20E-07	Tumor vs. Non-tumor	0.00090	0.73
				Low vs. Control	-0.019	0.0028
				High vs. Control	-0.0056	0.073
				High vs. Low	0.013	0.26

*Microarray β coefficients are intensity ratios of enriched: input. Ratios <1 indicate hypomethylation; ratios >1 indicate hypermethylation.
**Bisulfite sequencing β coefficients are derived from regression models. Coefficients <0 indicate hypomethyaltion; coefficients >0 indicate hypermethylation.

John Wiley & Sons, Inc.
This article is protected by copyright. All rights reserved.

Accepted Article

Table 4a. GO terms significantly enriched with differential methylation by tumor status.

Name	Comparison	#Genes	P-Value	FDR	Direction
middle ear morphogenesis	Tumor vs. No tumor	11	1.87E-08	4.64E-05	up
ear morphogenesis	Tumor vs. No tumor	51	8.84E-08	1.10E-04	up
embryonic organ morphogenesis	Tumor vs. No tumor	95	2.03E-07	1.68E-04	up
ear development	Tumor vs. No tumor	66	1.40E-06	8.69E-04	up
sensory organ development	Tumor vs. No tumor	169	2.20E-06	0.001091	up
embryonic organ development	Tumor vs. No tumor	142	6.39E-06	0.002641	up
hepaticobiliary system development	Tumor vs. No tumor	50	1.03E-05	0.003484	up
liver development	Tumor vs. No tumor	49	1.12E-05	0.003484	up
chordate embryonic development	Tumor vs. No tumor	248	4.52E-05	0.01126	up
embryo development ending in birth or egg hatching	Tumor vs. No tumor	250	4.54E-05	0.01126	up
inner ear morphogenesis	Tumor vs. No tumor	41	6.34E-05	0.014279	up
kidney development	Tumor vs. No tumor	62	1.58E-04	0.03268	up
brain development	Tumor vs. No tumor	205	1.76E-04	0.033418	up
demethylation	Tumor vs. No tumor	14	1.94E-04	0.033418	up
renal system development	Tumor vs. No tumor	65	2.02E-04	0.033418	up
covalent chromatin modification	Tumor vs. No tumor	116	2.46E-04	0.038055	up
metanephros development	Tumor vs. No tumor	21	2.65E-04	0.038651	up
histone modification	Tumor vs. No tumor	113	2.88E-04	0.039684	up
positive regulation of DNA repair	Tumor vs. No tumor	13	3.66E-04	0.046376	up
multicellular organism growth	Tumor vs. No tumor	44	3.77E-04	0.046376	up
organ morphogenesis	Tumor vs. No tumor	434	3.93E-04	0.046376	up
organ growth	Tumor vs. No tumor	40	4.12E-04	0.046376	up
positive regulation of cell-matrix adhesion	Tumor vs. No tumor	14	5.06E-04	0.054574	down
camera-type eye development	Tumor vs. No tumor	77	5.80E-04	0.059948	up

John Wiley & Sons, Inc.

This article is protected by copyright. All rights reserved.

Accepted Article

double-strand break repair	Tumor vs. No tumor	44	6.21E-04	0.061604	up
urogenital system development	Tumor vs. No tumor	91	7.21E-04	0.06416	up
regulation of the force of heart contraction	Tumor vs. No tumor	11	7.23E-04	0.06416	down
palate development	Tumor vs. No tumor	29	7.27E-04	0.06416	up
central nervous system neuron development	Tumor vs. No tumor	18	7.51E-04	0.06416	up
histone demethylase activity	Tumor vs. No tumor	10	9.82E-05	0.039075	up
demethylase activity	Tumor vs. No tumor	13	1.39E-04	0.039075	up
specific transcriptional repressor activity	Tumor vs. No tumor	26	5.12E-04	0.07352	up
protein methyltransferase activity	Tumor vs. No tumor	38	5.23E-04	0.07352	up

Table 4b. GO terms significantly enriched with differential methylation by BPA exposure level.

Name	Comparison	#Genes	P-Value	FDR	Direction
Golgi to plasma membrane transport	Low BPA vs. Control	10	1.23E-05	0.030447	up
macromolecule transmembrane transporter activity	Low BPA vs. Control	10	1.45E-04	0.040759	up
protein transmembrane transporter activity	Low BPA vs. Control	10	1.45E-04	0.040759	up
NADP or NADPH binding	Low BPA vs. Control	26	5.28E-04	0.098975	down
extrinsic to membrane	High BPA vs. Control	47	3.15E-05	0.006091	up
heterotrimeric G-protein complex	High BPA vs. Control	10	3.27E-05	0.006091	up
extrinsic to plasma membrane	High BPA vs. Control	26	3.25E-04	0.040366	up
acid-thiol ligase activity	High BPA vs. Control	13	5.11E-05	0.028725	up
sequence-specific DNA binding	High BPA vs. Control	424	1.53E-04	0.043107	up
sequence-specific DNA binding transcription factor activity	High BPA vs. Control	614	2.56E-04	0.04804	up
ligase activity, forming carbon-sulfur	High BPA vs. Control	22	4.02E-04	0.056521	up

John Wiley & Sons, Inc.

This article is protected by copyright. All rights reserved.

Accepted Article

bonds					
extrinsic to membrane	High BPA vs. Low BPA	47	3.15E-05	0.006091	up
heterotrimeric G-protein complex	High BPA vs. Low BPA	10	3.27E-05	0.006091	up
extrinsic to plasma membrane	High BPA vs. Low BPA	26	3.25E-04	0.040366	up
acid-thiol ligase activity	High BPA vs. Low BPA	13	5.11E-05	0.028725	up
sequence-specific DNA binding	High BPA vs. Low BPA	424	1.53E-04	0.043107	up
sequence-specific DNA binding transcription factor activity	High BPA vs. Low BPA	614	2.56E-04	0.04804	up
ligase activity, forming carbon-sulfur bonds	High BPA vs. Low BPA	22	4.02E-04	0.056521	up

John Wiley & Sons, Inc.

This article is protected by copyright. All rights reserved.

Accepted Article

Table 5. Pathway terms significantly enriched with differential methylation in BPA-exposed mice and/or with hepatic tumors

Name	Comparison	#Genes	P-Value	FDR	Direction
Acute Myocardial Infarction	Tumor vs. No tumor	14	6.24E-04	0.093603	up
Selenocompound metabolism	Low BPA vs. Control	13	1.28E-05	0.00258	up
African trypanosomiasis	Low BPA vs. Control	19	9.75E-04	0.098459	down
Role of Erk5 in Neuronal Survival	High BPA vs. Control	10	1.76E-04	0.026328	up
Histamine H2 receptor mediated signaling pathway	High BPA vs. Control	12	0.002505	0.039036	up
Beta3 adrenergic receptor signaling pathway	High BPA vs. Control	15	0.002672	0.039036	up
5HT4 type receptor mediated signaling pathway	High BPA vs. Control	16	0.002882	0.039036	up
Endogenous cannabinoid signaling	High BPA vs. Control	13	0.002974	0.039036	up
Cortocotropin releasing factor receptor signaling pathway	High BPA vs. Control	17	0.002982	0.039036	up
Heterotrimeric G-protein signaling pathway-rod outer segment phototransduction	High BPA vs. Control	19	0.003299	0.039036	up
5HT1 type receptor mediated signaling pathway	High BPA vs. Control	20	0.004139	0.039036	up
Beta1 adrenergic receptor signaling pathway	High BPA vs. Control	23	0.004662	0.039036	up
Beta2 adrenergic receptor signaling pathway	High BPA vs. Control	24	0.005096	0.039036	up
GABA-B receptor II signaling	High BPA vs. Control	18	0.005347	0.039036	up
Metabotropic glutamate receptor group II pathway	High BPA vs. Control	27	0.008168	0.047157	up
Histamine H1 receptor mediated signaling pathway	High BPA vs. Control	27	0.008371	0.047157	up
Oxytocin receptor mediated signaling pathway	High BPA vs. Control	35	0.009135	0.047157	up
Muscarinic acetylcholine receptor 1 and 3 signaling pathway	High BPA vs. Control	34	0.010031	0.047157	up
Metabotropic glutamate receptor group III pathway	High BPA vs. Control	39	0.010058	0.047157	up
PI3 kinase pathway	High BPA vs. Control	30	0.010336	0.047157	up

John Wiley & Sons, Inc.

This article is protected by copyright. All rights reserved.

5HT2 type receptor mediated signaling pathway	High BPA vs. Control	37	0.011884	0.04919	up
Thyrotropin-releasing hormone receptor signaling pathway	High BPA vs. Control	36	0.012129	0.04919	up
Muscarinic acetylcholine receptor 2 and 4 signaling pathway	High BPA vs. Control	34	0.014209	0.054593	up

Figure Legends

Figure 1. Overlapping mouse and human genes altered by BPA exposure in the Jak-Stat signaling pathway Unique mouse microarray gene IDs involved in Jak/Stat signaling that overlap with human JAK/STAT gene IDs with known interactions with BPA in The Comparative Toxicogenomics Database are shown in red.

Figure 2. Overlapping mouse and human genes altered by BPA exposure in the Mapk signaling pathway. Unique mouse microarray gene IDs involved in Mapk signaling that overlap with human MAPK gene IDs with known interactions with BPA in The Comparative Toxicogenomics Database are shown in red.

Accepted Article

John Wiley & Sons, Inc.

This article is protected by copyright. All rights reserved.

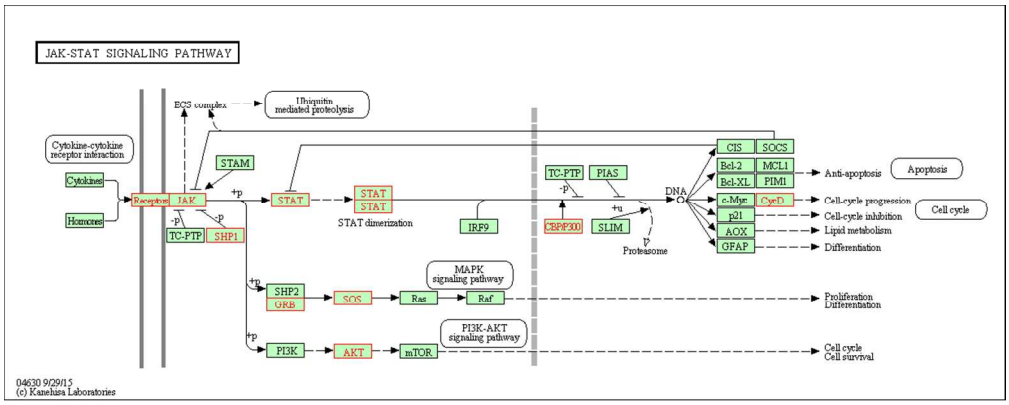

Figure 1. Overlapping mouse and human genes altered by BPA exposure in the Jak-Stat signaling pathway Unique mouse microarray gene IDs involved in Jak/Stat signaling that overlap with human JAK/STAT gene IDs with known interactions with BPA in The Comparative Toxicogenomics Database are shown in red.
434x171mm (72 x 72 DPI)

Accepted

This article is protected by copyright. All rights reserved.

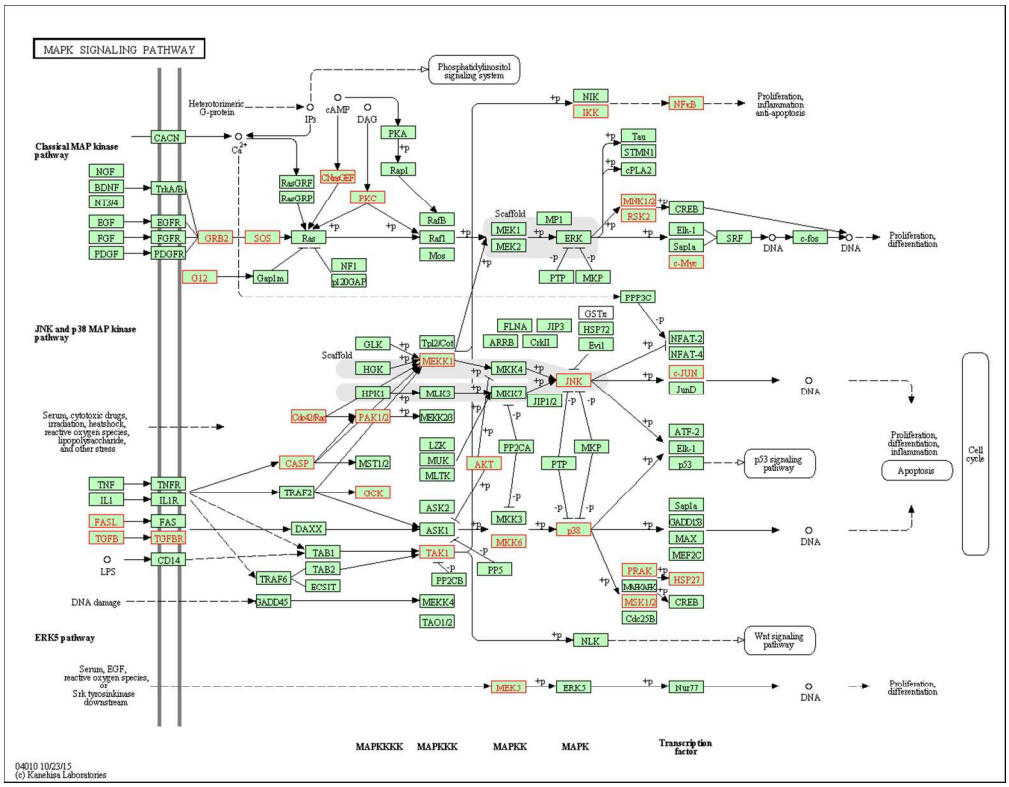

Figure 2. Overlapping mouse and human genes altered by BPA exposure in the Mapk signaling pathway. Unique mouse microarray gene IDs involved in Mapk signaling that overlap with human MAPK gene IDs with known interactions with BPA in The Comparative Toxicogenomics Database are shown in red.
473x367mm (72 x 72 DPI)

Accep

This article is protected by copyright. All rights reserved.